EXPERIMENTAL CHARACTERIZATION OF SLURRY BUBBLE-COLUMN REACTOR HYDRODYNAMICS

Kim A. Shollenberger[1]
e-mail: kasholl@sandia.gov
phone: (505) 844-5823
FAX: (505) 844-8251

Nancy B. Jackson[2]
e-mail: nbjacks@sandia.gov
phone: (505) 844-0940
FAX: (505) 845-9500

John R. Torczynski[1]
e-mail: jrtorcz@sandia.gov
phone: (505) 845-8991
FAX: (505) 844-8251

Timothy J. O'Hern[1]
e-mail: tjohern@sandia.gov
phone: (505) 844-9061
FAX: (505) 844-8251

[1]Engineering Sciences Center
[2]Advanced Energy Technology Center
Sandia National Laboratories
Albuquerque, NM 87185-5800 USA

ABSTRACT

Sandia's program to develop, implement, and apply diagnostics for hydrodynamic characterization of slurry bubble-column reactors (SBCRs) at industrially relevant conditions is discussed. Gas-liquid flow experiments are performed on an industrial scale. Gamma-densitometry tomography (GDT) is applied to measure radial variations in gas holdup at one axial location. Differential pressure (DP) measurements are used to calculate volume-averaged gas holdups along the axis of the vessel. The holdups obtained from DP show negligible axial-variation for water but significant variations for oil, suggesting that the air-water flow is fully developed (minimal flow variations in the axial direction) but that the air-oil flow is still developing at the GDT measurement location. The GDT and DP gas holdup results are in good agreement for the air-water flow but not for the air-oil flow. Strong flow variations in the axial direction may be impacting the accuracy of one or both of these techniques. DP measurements are also acquired at high sampling frequencies (250 Hz) and are interpreted using statistical analyses to determine the physical mechanism producing each frequency component in the flow. This approach did not yield the information needed to determine the flow regime in these experiments. As a first step toward three-phase material-distribution measurements, electrical-impedance tomography (EIT) and GDT are applied to a liquid-solid flow to measure solids holdup. Good agreement is observed between both techniques and known values.

INTRODUCTION

In the Fischer-Tropsch approach to indirect liquefaction, slurry bubble-column reactors (SBCRs) are used to convert coal syngas into a desired product. However, gas distribution nonuniformity can cause buoyancy-driven flow, which reduces gas residence time and process efficiency. Thus, it is essential to characterize three-phase flow phenomenology, particularly as affected by gas flow rate, slurry thermophysical properties, sparger geometry, and reactor diameter. To this end, Sandia is developing, implementing and applying diagnostics for hydrodynamic characterization of SBCRs at industrially relevant conditions [1-4].

EXPERIMENTAL SETUP AND TECHNIQUES

An SBCR apparatus has been constructed as a testbed for diagnostics development and data acquisition under industrially relevant conditions. The SBCR vessel, shown in Figure 1 [1], is stainless steel and has a 0.48 m ID (comparable to the LaPorte Alternative Fuels Development Unit, AFDU), a 3-m height, and a 1.27-cm thick wall. It can operate at pressures up to 100 psig (0.69 MPa) and temperatures up to 200 °C, achievable via an in-line gas heater and external vessel heaters controlled at four vertical locations. Two instrumentation ports and two viewports are centered at six vertical positions 0.457 m apart. Validyne variable reluctance differential pressure (DP) transducers are mounted at each of these positions to measure the vertical pressure gradient, from which the average gas volume fraction between adjacent transducers can be inferred. The transducers are configured to measure pressures ranging from 0-5 psid (0.035 MPa) with an accuracy of 0.003 psid (10^{-5} MPa) at a maximum frequency response of 5 kHz.

Sandia is a multiprogram laboratory operated by Sandia Corporation, a Lockheed Martin Company, for the United States Department of Energy under Contract DE-ACO4-94AL85000

DISCLAIMER

The SBCR testbed is operated in the following manner. Prior to operation, the vessel is partially filled with liquid to a height of four diameters. Two liquids have been used thus far: water and Drakeol 10, a lightweight mineral oil used at the AFDU for methanol production. Air is then injected through one of several interchangeable spargers near the bottom of the vessel. The current sparger is a 0.15-m diameter ring formed from 1.1 cm ID stainless steel tubing with twelve 0.3175-cm diameter holes in the top surface. By regulating the gas flow out of the top of the SBCR, the head space pressure is fixed within the vessel at a prescribed value. To date, gas superficial velocities up to 0.4 m/s, gas volume fractions or gas holdups up to 0.4, and pressures up to 54 psia (0.37 MPa) have been examined in the SBCR vessel.

A gamma-densitometry tomography (GDT) system, consisting of a 5-Curie Cs-137 gamma source, a NaI scintillation detector mounted on opposing arms of a two-axis computer-controlled traverse, and axisymmetric tomographic reconstruction software, has been implemented [2]. GDT measures the distribution of the attenuation coefficient of gamma photons, which is linearly related to the gas volume fraction distribution. For gas-liquid-solid flows, such as slurry Fischer-Tropsch, additional information is needed beyond GDT to determine the distribution of all three phases. Electrical-impedance tomography (EIT) can potentially provide this. In EIT, electrodes are placed around the vessel's inner perimeter. Current flows between two electrodes, and the resulting voltages are measured at the remaining electrodes. A reconstruction algorithm uses the measured voltages to determine the electrical conductivity distribution, which is related to the distribution of the phases. EIT electronics, hardware, and software have been implemented for validation experiments [3] and for liquid/solid flows [4]. The EIT hardware consists of a 0.19-m diameter Lucite cylinder with 16 point electrodes (3-mm diameter) mounted on its inner surface, a stabilized 50 kHz constant current source, and electrical hardware to condition and sample voltages. A three-dimensional finite element reconstruction technique developed at Sandia called FEMEIT [3-4] is applied to determine the electrical conductivity distribution.

GAS-HOLDUP AXIAL VARIATION RESULTS

To understand the limitations inherent in the GDT and DP techniques and to better understand flow development near the sparger, axial variations in gas holdup were measured in the SBCR using the DP technique. Figure 2 shows results for both air-water and air-oil flows. The radially averaged gas holdup results obtained at $L/D = 2$ from GDT measurements are also shown using closed symbols. The air-water results show that the gas holdup is uniform in the column, except near the top interface, and that GDT agrees well with the DP results. For air-oil, the results show that there is a significant variation in gas holdup along the column and that GDT results are significantly lower than DP results for all three cases. The axial variation in gas holdup suggests that the air-oil flow is still developing (there are significant flow variations in the axial direction) which may impact the accuracy of one or both of these techniques. In particular, calculations of gas holdup from DP data are made using a steady-state hydrostatic equation, the applicability of which is suspect for a developing flow. Thus, predictions of gas holdup from DP may be less accurate near the sparger or within the region of developing flow.

PRESSURE-FLUCTUATION RESULTS

Experiments were performed in Sandia's SBCR testbed to assess the applicability of the Delft [5] pressure-fluctuation technique to determine flow regimes under industrially relevant conditions. Fourier and statistical techniques are applied to pressure histories to determine the dominant frequencies and whether pressure histories at different stations are correlated at some of these dominant frequencies. Pressure histories were acquired in the SBCR testbed for superficial gas velocities up to 0.24 m/s and head space pressures up to 57 psia (0.393 MPa) using air-oil. The pressure histories contained 10,000 points each and were sampled at a frequency of 250 Hz (all dominant frequencies observed by the Delft group are well below this value). Although the data acquisition system is capable of sampling at rates up to 20,000 Hz, a lower sampling frequency was chosen to ensure measurement stability and to improve accuracy by oversampling the transducers.

Figure 3 shows Fourier-transform results at two superficial gas velocities and two head space pressures obtained at $L/D = 1.3$. The Fourier transforms at all other axial locations did not differ significantly from these results and are not shown. Two dominant frequencies (peaks) are observed in each plot. The first peak is at a very low frequency of approximately 1 Hz and is not clearly resolved because the duration of each record is only 40 seconds. The second peak has a frequency of about 5-25 Hz and is well resolved. Unlike the Delft results, no appreciable peaks are observed with frequencies around 100 Hz. These two dominant peaks are observed to have the following dependence on flow conditions. As the superficial gas velocity is increased, the peak amplitudes increase, and the peak frequencies decrease. As the head space pressure is increased, the peak amplitudes

decrease, and the peak frequencies increase. These peak-frequency trends are summarized in Figure 4, which shows the location of the peak frequency in the 5-25 Hz range as a function of superficial gas velocity and pressure. Examination of the coherence between pressure histories at different pressure taps shows that both of the dominant peaks in the Fourier transforms are highly correlated between different pressure taps, suggesting that these two frequencies correspond to global phenomena.

One source of global, correlated pressure waves is the formation and release of individual bubbles from the sparger. Davidson and Schuler [6] proposed a correlation for the frequency of bubble formation from an upward-facing orifice with a high gas flow rate into a low-viscosity liquid at atmospheric pressure in terms of the gravitational acceleration and the volumetric flow rate. This correlation is also shown on Figure 4. The close agreement between the correlation and the low-pressure data suggest that bubble formation at the sparger is the source of this frequency peak. Although no correlation for bubble-formation frequency as a function of pressure could be found, LaNauze and Harris [7] observed that an increase in pressure causes smaller but more numerous bubbles to be formed at an orifice. This suggests that the peak frequency should increase and the peak amplitude should decrease as pressure is increased, in accord with the experimental data shown in Figures 3-4.

Figure 5 shows the standard deviation of the pressure histories as a function of superficial gas velocity and pressure. The standard deviation increases with increasing superficial gas velocity but decreases slightly with increasing head space pressure. These trends can be explained in terms of the effects of these parameters on the size of bubbles being formed. It is generally accepted that the bubble size increases as the gas flow rate is increased. The formation of larger bubbles should result in higher magnitude pressure fluctuations and standard deviations, as observed. Similarly, the smaller bubbles formed at higher pressures, as documented by LaNauze and Harris [7], should result in lower magnitude pressure fluctuations and standard deviations, as observed.

ELECTRICAL-IMPEDANCE TOMOGRAPHY RESULTS

To assess the suitability of EIT to provide the additional information needed for three-phase measurements, GDT and EIT have both been applied to a liquid-solid flow [4]. The experimental setup, shown in Figure 6, consisted of a cylinder (0.19-m diameter) filled with water, in which 80 μm glass spheres were suspended by a mixer to achieve three different solid volume fractions. Figure 7 shows the radial variation of solid volume fraction obtained using GDT. Both GDT and EIT revealed a relatively uniform distribution of solids in the measurement plane. The radially averaged solid volume fractions determined by GDT and EIT are seen to be in close agreement with each other for all cases (see Figure 8) and with the nominal values for the first two cases. The third case is interesting in that the GDT and EIT values are in agreement with each other but are significantly higher than the nominal value. It was observed visually that the mixing was not strong enough to produce a uniform axial distribution of glass spheres throughout the cylinder for a nominal solid volume fraction of 0.03, so the solid volume fraction was less than the nominal value near the top of the cylinder and larger at the measurement plane below.

CONCLUSIONS

Gas holdup measurements have been made for a range of flow conditions and for both water and Drakeol 10 in the SBCR. GDT provides radially resolved measurements, and DP provides axially resolved measurements. A comparison of results from these two techniques indicated a significant discrepancy in the presence of significant axial variation. Additional concerns were raised over the length of the developing region for oil. Pressure-fluctuation techniques were investigated but were not found to be capable of predicting flow-regime transitions for air-oil flows in the industrial-scale SBCR testbed. EIT was demonstrated as a suitable technique for measuring modest concentrations of a uniformly dispersed solid phase, as required for three-phase measurements. Future work will focus on clarifying the effect of flow development on the accuracy of GDT and DP, determining why the pressure-fluctuation results for air-oil experiments in the SBCR testbed differed from the Delft air-water results, and extending EIT to large, nonuniformly disperse solids loadings.

ACKNOWLEDGEMENTS

Sandia is a multiprogram laboratory operated by Sandia Corporation, a Lockheed Martin Company, for the United States Department of Energy under Contract DE-ACO4-94AL85000. The excellent technical support provided by Thomas W. Grasser, John J. O'Hare, John Henfling, and C. Buddy Lafferty is highly appreciated. The authors gratefully acknowledge many interactions with Bernard A. Toseland and Bharat L. Bhatt of Air Products and Chemical, Inc.

REFERENCES

1. J. R. Torczynski, T. J. O'Hern, D. R. Adkins, N. B. Jackson, & K. A. Shollenberger, "Advanced Tomographic Flow Diagnostics for Opaque Multiphase Fluids," *SAND REPORT*, SAND97-1176, 1997.
2. K. A. Shollenberger, J. R. Torczynski, D. R. Adkins, T. J. O'Hern, & N. B. Jackson, "Gamma-Densitometry Tomography of Gas Holdup Spatial Distribution in Industrial-Scale Bubble Columns," *Chem.Eng. Sci.*, **52**, 2037-2048, 1997.
3. J. R. Torczynski, T. J. O'Hern, K. A. Shollenberger, S. L. Ceccio, & A. L. Tassin, "Finite Element Method Electrical Impedance Tomography for Phase Distribution Determination in Multiphase Flows: Validation Calculations and Experiments," in *Cavitation and Multiphase Flow Forum*, J. Katz & K. J. Farrell, eds., FED-Vol. 236, 497-501, 1996.
4. K. A. Shollenberger, J. R. Torczynski, T. J. O'Hern, D. R. Adkins, S. L. Ceccio, & D. L. George, "Comparison of Gamma-Densitometry Tomography and Electrical Impedance Tomography for Determining Material Distribution in Liquid-Solid Flows," in *Cavitation and Multiphase Flow Forum*, J. Katz & K. J. Farrell, eds., FEDSM97-3690, 1997.
5. H. M. Letzel, J. C. Schouten, R. Krishna, & C. M. van den Bleek, "Characterization of Regimes and Regime Transitions in Bubble Columns by Chaos Analysis of Pressure Signals," *Chem.Eng. Sci.*, in press, 1997.
6. J. F. Davidson & B. O. G. Schuler, "Bubble Formation at an Orifice in a Viscous Liquid," *Trans. Inst. Chem. Eng.* **38**, 144-154, 1960.
7. R. D. LaNauze & I. J. Harris, "Gas Bubble Formation at Elevated System Pressures," *Trans. Inst. Chem. Eng.* **52**, 337-348, 1974.

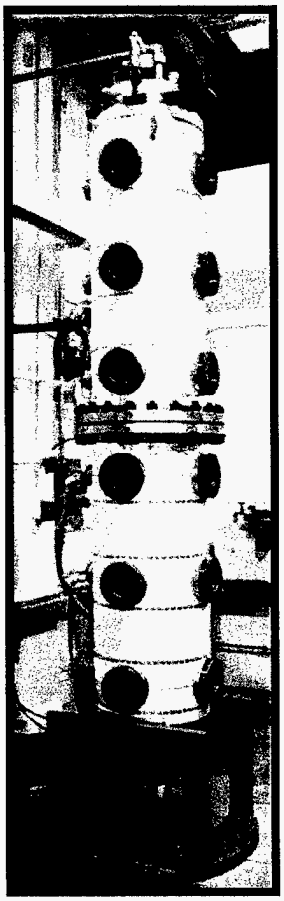

Figure 1. Sandia's slurry bubble-column reactor (SBCR) vessel (0.48-m ID, 3-m height, pressures to 100 psig, temperatures to 200 °C, high gas flow rates).

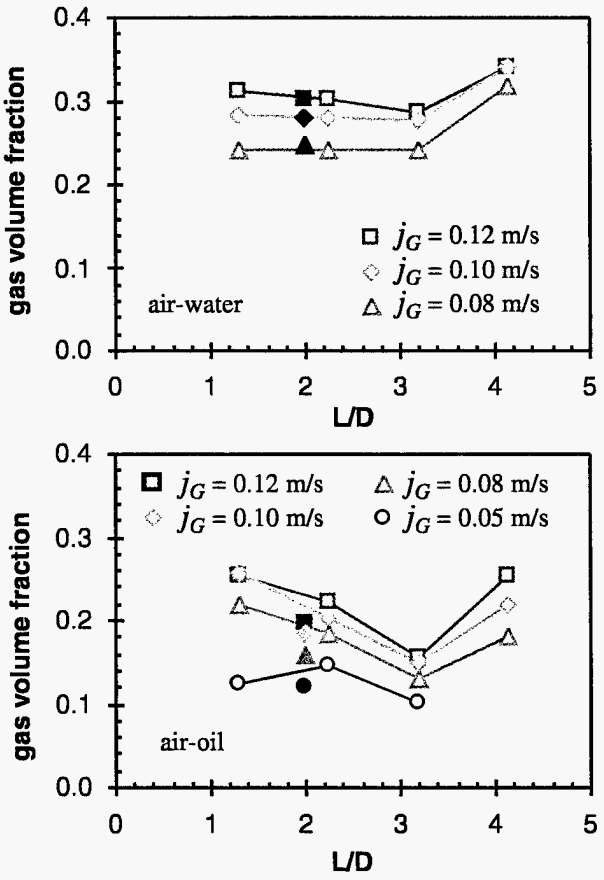

Figure 2. Axial variation of gas volume fraction as a function of superficial gas velocity at 42 psia (0.29 MPa). Open symbols are DP data and closed symbols are GDT data.

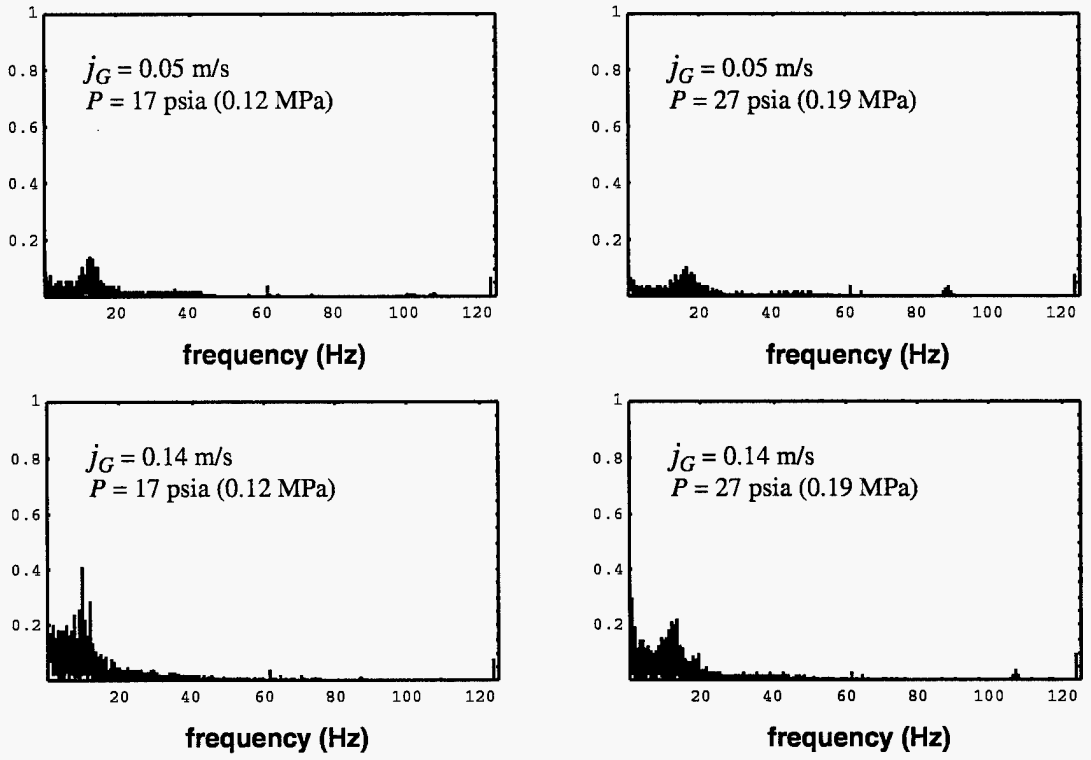

Figure 3. Magnitude of Fourier transform of pressure histories (10,000 points at 250 Hz) at L/D = 1.3 in the SBCR testbed for various superficial gas velocities and head space pressures.

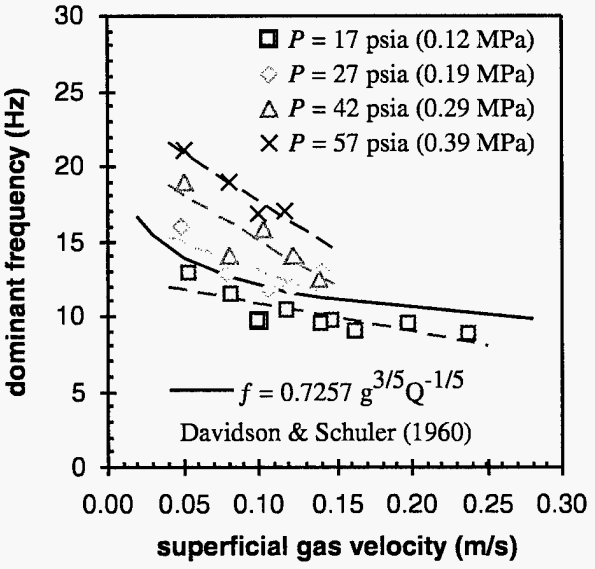

Figure 4. Dominant frequency of pressure fluctuations (in the 5-25 Hz range) as a function of superficial gas velocity and head space pressure in SBCR with air-oil flow.

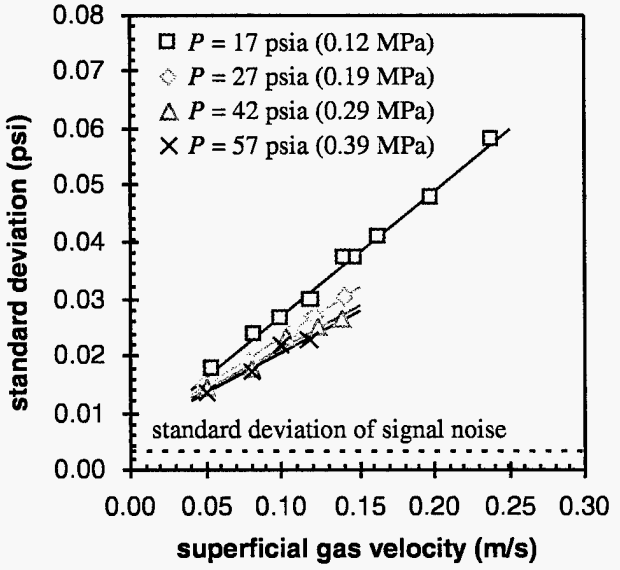

Figure 5. Standard deviation of pressure signals as a function of superficial gas velocity and head space pressure in SBCR with air-oil flow.

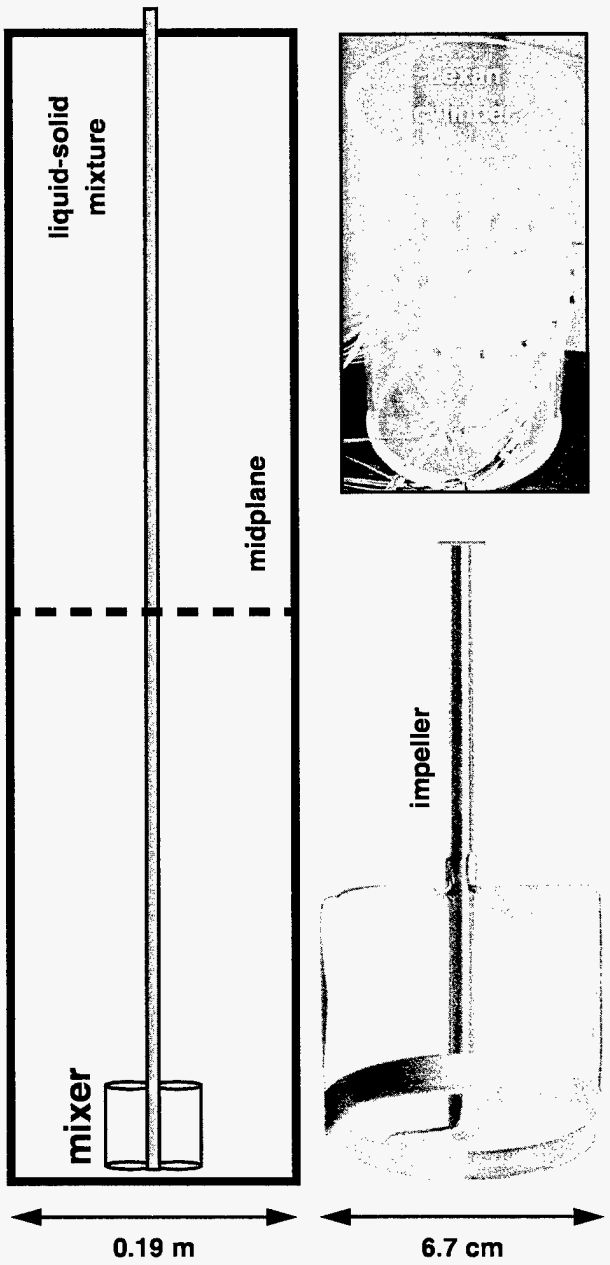

Figure 6. Left, liquid-solid-flow experiment. Top right, Lexan cylinder without mixer but with EIT electrodes. Bottom right, impeller.

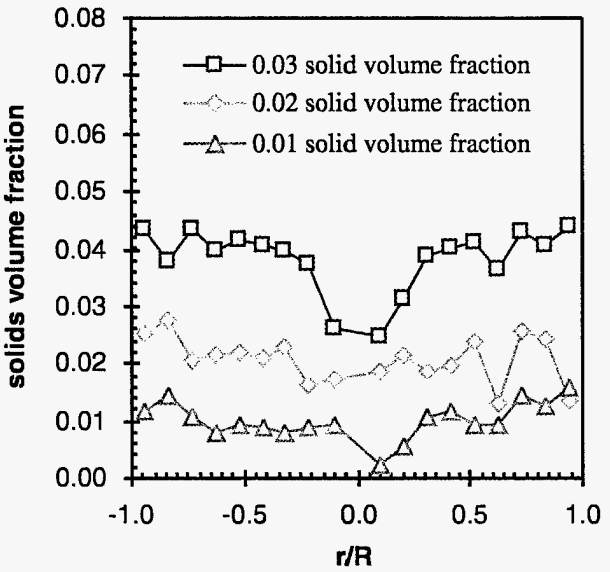

Figure 7. Radial variation of chordal-averaged solid volume fractions from GDT.

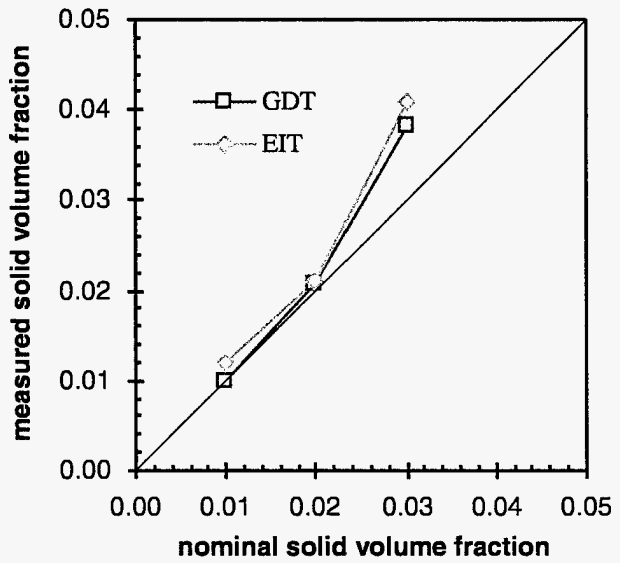

Figure 8. Radially averaged solid volume fractions from GDT and EIT at L/D = 2 compared to the nominal (volume-averaged) solid volume fraction.

Report Number (14) SAND--97-1924C
CONF-970973--

Publ. Date (11) 199709
Sponsor Code (18) DOE/FE,XF
UC Category (19) UC-101,DOE/ER

DOE